Theor Chem Acc (2011) 130:507–513
DOI 10.1007/s00214-011-1035-4

REGULAR ARTICLE

The concerted and stepwise chemisorption mechanisms of isothiazole and thiazole on Si(100)−2 × 1 surface

Manik Kumer Ghosh · Cheol Ho Choi

Received: 12 February 2011 / Accepted: 29 August 2011 / Published online: 15 September 2011

Abstract The surface reaction pathways of isothiazole and thiazole on Si(100)−2 × 1 surface were theoretically investigated using multireference wavefunctions. In the case of isothiazole, the Si–N dative adduct turned out to be the major surface product. In contrast, a direct reaction competition between a concerted $[4 + 2]_{CC}$ cycloaddition and Si–N dative adduct was found in the adsorption of thiazole. Therefore, it is concluded that the particular geometric arrangements of heteroatoms exhibit distinctly different initial surface reaction mechanisms.

Keywords Surface reaction · Quantum calculation · Isothiazole and thiazole

1 Introductions

Cycloaddition reaction has been a very important class of surface reactions in the surface adsorptions on silicon [1–3]. Although the direct addition of a single C = C π-bond to the Si dimer on the Si(100) surface constitutes the orbital symmetry-forbidden 2s + 2s cycloaddition [4], early experimental [5–8] and theoretical [9–11] studies have shown that the unsaturated hydrocarbons, such as acetylene, ethylene, and propylene, can readily react with Si(100) surface yielding [2 + 2] products. However, there has been a controversy [12, 13] over the stereochemistry of the reactions. The two most likely reaction pathways of alkene adsorption are a π-complex and a diradical channels. The π-complex channel can be described by a three-atom intermediate, in which the stereochemistry should be retained as the alkene approaches to the Si dimer. Therefore, the π-complex channel is stereospecific. On the other hand, the diradical channel can be described by a Si–C single-bonded diradical intermediate. Once the alkene π-bond is broken, rotation around the C–C σ-bond is possible, resulting in a loss of stereospecificity, if it occurs before the second Si–C bond is formed. According to a comparative theoretical study [14] of the adsorptions of ethylene and 2-butene on Si(100), both the diradical and the π-complex pathway were found. Since the net reaction barriers of the channels are similar, it was concluded that the final distributions of surface products may depend on the experimental kinetic environment as well as substituents. In any event, these diradical and π-complex channels of [2 + 2] cycloadditions constitute an asymmetric stepwise path.

Diene systems have also been actively studied. Pioneering theoretical and experimental studies have shown [15–17] that the surface dimer can act as a good dienophile yielding 'Diels–Alder'-like [4 + 2] cycloaddition products, in which a conjugated diene reacts with the silicon surface dimer to form a six-membered ring. A subsequent experiment by Hamers and coworkers [18] supported the observation. However, they noted a minor [2 + 2] product as well, strongly indicating the existence of competition between [4 + 2] and [2 + 2] reactions in the adsorption of diene on the Si(100) surface. Theoretical studies by Choi and Gordon [19] support for the existence of competing reactions by showing that there exists a low-energy [2 + 2] cycloaddition pathway in addition to the [4 + 2] path. They also showed that the [4 + 2] channel is concerted

Dedicated to Professor Shigeru Nagase on the occasion of his 65th birthday and published as part of the Nagase Festschrift Issue.

M. K. Ghosh · C. H. Choi (✉)
Department of Chemistry, College of Natural Sciences, Kyungpook National University, Taegu 702-701, South Korea
e-mail: cchoi@knu.ac.kr

contrasting to the stepwise path of [2 + 2]. Cycloaddition can also be found in the adsorptions of aromatic molecules. The aromatic benzene [20–31] can easily adsorb on Si(100) surface via concerted [4 + 2] path. Theoretical study on benzene adsorption with multireference methods [29] showed that although the [4 + 2], [2 + 2], and tetra-σ-bonded products are possible, the [4 + 2] product is thermodynamically the most stable and kinetically the most easily accessible. Unlike conjugated dienes, it appears that benzene selectively prefers [4 + 2] cycloaddition reaction on the Si(100) surface.

It is interesting to note that the mechanism of [4 + 2] cycloaddition can be significantly altered when substituents are introduced. In the theoretical study of acrylonitrile on the Si(100)−2 × 1 surface [32], it was reported that a stepwise [4 + 2] types of reaction occur by way of dative-bond intermediate in which the nitrogen lone pair of acrylonitrile initially forms a stable bond with the surface Si dimer. The stepwise [4 + 2] channel can also be implied in the case of pyridine adsorption on Si(100). On the basis of TDS (thermal desorption spectroscopy), XPS, HREELS (electron energy loss spectroscopy), and DFT calculations [33], the dative-bonded pyridine through the lone pair electrons of N and [4 + 2]-like cycloadduct with two σ-linkages of Si–N and Si–C on Si(100) were reported. The latter product implies a stepwise path of [4 + 2] addition, since one of the σ-linkages is Si–N bond. It was shown that the adsorptions of aromatic isoxazole and thiazole [34] on Si(111) surface yield dative-bond addition and [4 + 2]-like cycloaddition. On the other hand, the adsorptions of oxazole on the same surface yield dative-bond addition and [2 + 2]-like cycloaddition. All of these products contain one Si–N surface bond, indicating that they share the same dative-bond intermediate in their reaction mechanisms. These studies on heterogeneous aromatic systems inherently assume that the overall reactions are stepwise and dative-bond formation precedes cycloadditions. So the cycloaddition reactions only occur afterward, implying no direction reaction competition between the dative addition and the cycloaddition. However, the concerted [4 + 2] cycloaddition is well known to have very small or near zero reaction barriers. Therefore, in some particular conditions, the concerted [4 + 2] cycloaddition can be directly formed without the dative-bonded precursor state. Theoretical mechanism study can be helpful to clarify this.

Unlike common conjugated molecules, isothiazole and thiazole show considerable aromaticity; also unlike benzene, it has inhomogeneous electron distribution and two heteroatoms with lone pair electrons. For formulation of an aromatic π-conjugation of $4n + 2$ electrons, the sulfur atom and nitrogen atom contribute two and one electrons, respectively. Because these molecules contain both an aromatic ring and lone pair electrons, the molecules are expected to form a variety of adsorption states with silicon surface via either cycloaddition reaction or dative bonding Lewis base–acid reaction. In this paper, the initial potential energy surfaces of these molecules on Si(100)−2 × 1 surface were theoretically explored to obtain the detailed reaction mechanisms.

2 Computational details

All electron 6-31G(d) [35] basis set was used throughout this work. Minimum energy reaction paths were determined by first optimizing the geometries of minima and transition states. Then, each stationary point was characterized by computing and diagonalizing the Hessian matrix (matrix of energy second derivatives). Various points on the reaction paths, particularly transition states and intermediates, are often inherently multiconfiguration especially in the case of cycloadditions. Therefore, CASSCF (complete active space SCF) wavefunctions [36–40] were used to describe entire potential energy surfaces. For the study of adsorption and chemisorption of isothiazole and thiazole on the Si(100)−2 × 1 surface, individual sets of active spaces were used for each channel shown in Table 1.

In order to recover the dynamic electron correlation and to ensure that all parts of the reaction path are treated equivalently, multireference second-order perturbation theory was used [41, 42]. The particular version of this method used in the present work is referred to as MRMP2 (multireference second-order perturbation theory) [43, 44]. The relative energies will focus on the MRMP2 values obtained at the MCSCF geometries (MRMP2//MCSCF). The GAMESS (general atomic and molecular electronic structure system) [45, 46] program was used for all of the computations.

In order to include surface size effects, a hybrid quantum mechanics/molecular mechanics (QM/MM) method called SIMOMM [47] was adopted. In this work, the QMMM models were designed such that $C_3SNSi_9H_{15}$ quantum region embedded in $C_3SNSi_{48}H_{39}$ cluster, for both thiazole and isothiazole. All figures show only the QM region for clarity. The chemically inactive region of the system is calculated by computationally inexpensive force field methods, while the chemically active part is treated by quantum mechanics. It has been shown that the SIMOMM (surface integrated molecular orbital molecular mechanics) QM/MM method gives reasonable results at relatively low computational cost [1]. The SIMOMM method has been used successfully to study many different adsorbates on Si(100)−2 × 1 surface [48–57], as well as the Si(111)−7 × 7 reconstructed surface [58], the SiC(100) surface [59], and the diamond(100) surface [60]. MM3 [61–63] parameters were used for the molecular mechanics part of

Table 1 Design of CASSCF active spaces of various reaction channels

Reaction channel	Active space size	Construction
Si–N and Si–S dative-bonded adducts (Fig. 1)	(8,5)	Two electrons in the π and π^* orbitals of surface Si dimer + two electrons in the one nonbonding orbitals of nitrogen + four electrons in the two nonbonding orbitals of sulfur.
$[2 + 2]_{NC}$ cycloaddition reaction (Fig. 2)	(6,5)	Two electrons in the π and π^* orbitals of surface Si dimer + two electrons in the π and π^* orbitals of N = C bond + two electrons in the one nonbonding orbitals of nitrogen.
$[2 + 2]_{CC}$ cycloaddition reaction (Fig. 3)	(4,4)	Two electrons in the π and π^* orbitals of surface Si dimer + two electrons in the π and π^* orbitals of C = C bond.
[4 + 2] cycloaddition reaction (Fig. 4)	(8,7)	Two electrons in the π and π^* orbitals of surface Si dimer + two electrons in the π and π^* orbitals of N = C bond + two electrons in the π and π^* orbitals of C = C bond + two electrons in the one nonbonding orbitals of nitrogen.
Ring-opening reaction of isothiazole (Fig. 5)	(10,7)	Two electrons in the π and π^* orbitals of surface Si dimer + two electrons in the σ and σ^* orbitals of N–S bond + two electrons in the one nonbonding orbitals of nitrogen + four electrons in the two nonbonding orbitals of sulfur.

the computations. All of the computations were done without imposing symmetry unless otherwise specified.

3 Results and discussions

Due to the two heteroatoms of thiazole and isothiazole, several surface binding configurations are possible. According to our calculations, $[2 + 2]_{NC}$, $[2 + 2]_{CC}$, $[4 + 2]_{NC}$, and $[4 + 2]_{CC}$ cycloaddition products were found, where the subscript NC represents that one of the surface σ-bond is Si–N. The subscript CC emphasizes two Si–C surface σ-bonds.

3.1 Dative-bonded adducts

As in the cases of the pyridine [33], pyrazine [64], and 1-pyrazoline [65], the N–Si dative-bonded adducts were found in the initial adsorptions of isothiazole and thiazole on the Si(100)−2 × 1 surface (see Fig. 1). They are represented in the Figure as $I_{isot}1$ and $I_{thia}1$, respectively. This end-on chemisorption occurs barrierlessly through a nucleophilic attack of the N lone pairs to the positively charged Si atom of the surface dimer. The stabilization energies of these Si–N dative-bonded adduct species are 23.6 and 20.6 kcal/mol for $I_{isot}1$ and $I_{thia}1$, respectively, at the MRMP2//CASSCF(8,5)/6-31G(d) level of theory. These values are in good agreements with those of pyridine [33], pyrazine [64], and 1-pyrazoline [65].

In addition to Si–N dative-bonded adduct, Si–S dative-bond adducts $I_{isot}2$ and $I_{thia}2$ have been also observed in isothiazole and thiazole adsorption, respectively (see Fig. 1). In the $I_{isot}2$ and $I_{thia}2$, the S atom of isothiazole and thiazole is linked with the buckled-down Si atom of the surface dimer, with a Si–S distances of 2.58 and 2.57 Å, respectively. Unlike the Si–N adducts were the adsorbed

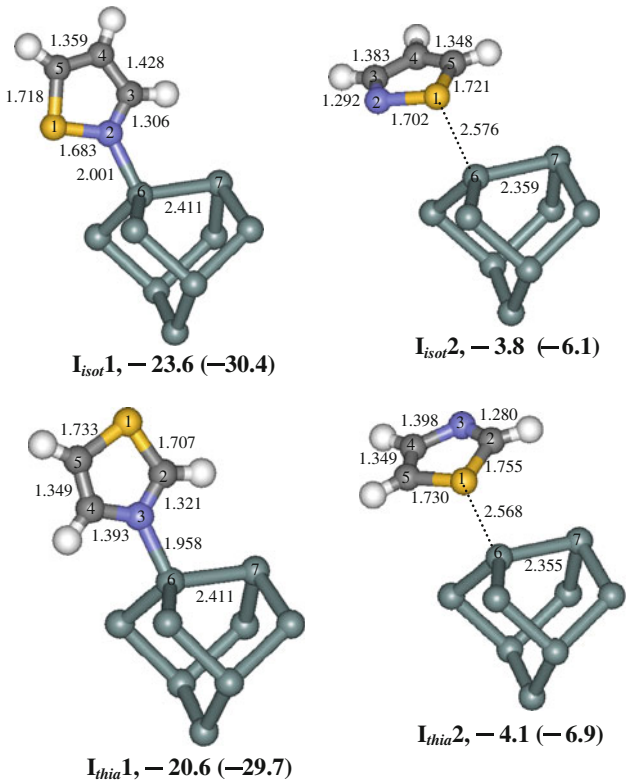

Fig. 1 The structures of the Si–N and Si–S dative-bond adducts. Relative energies are obtained with SIMOMM:MRMP2/6-31G(d). The values in *parentheses* are obtained with SIMOMM:CASSCF/6-31G(d). Geometric data are from the CASSCF results

molecular planes are normal to the surface, those of isothiazole and thiazole were nearly parallel with the surface. These Si–S adducts are slightly exothermic by 3.8 and 4.1 kcal/mol relative to the reactants, respectively. So Si–S adducts are in general less stable than the corresponding Si–N adducts. The same chemisorption state (Si–S dative-bond) also has been observed in the case of thiophene [66]

on the Si(100) surface with the similar stabilization energy 2.9 kcal/mol. In short, the Si–N adducts are the most important initial surface species in both isothiazole and thiazole.

3.2 Direct and indirect [2 + 2] cycloaddition reaction channels

Whether the cycloaddition occurs as a subsequent surface reaction from the Si–N dative adducts or as a direct concerted reaction from the reactants is one of the main issues. According to our calculations, both channels are possible.

3.2.1 Stepwise mechanism of [2 + 2]$_{NC}$ products

In both the isothiazole and thiazole, the $[2 + 2]_{NC}$ products are formed by way of Si–N dative-bond adducts constituting a stepwise [2 + 2] cycloaddition mechanism. In the case of isothiazole (see Fig. 2), the $[2 + 2]_{NC}$ transition state ($TS_{isot}1$) connects the stable Si–N adduct($I_{isot}1$) and the $[2 + 2]_{NC}$ product($P_{isot}1$) with the reaction barrier of 9.7 kcal/mol. And the finally formed $[2 + 2]_{NC}$ product($P_{isot}1$) is more stable than the reactant by 7.3 kcal/mol. The similar stepwise reaction to $[2 + 2]_{NC}$ product($P_{thia}1$) is also found in the case of thiazole (see Fig. 2). The $[2 + 2]_{NC}$ transition state ($TS_{thia}1$) connects the initial Si–N adduct($I_{thia}1$) and the $[2 + 2]_{NC}$ product($P_{thia}1$) with the barrier height of 6.9 kcal/mol. The reaction barriers of these two $[2 + 2]_{NC}$ transition states are not prohibitively large. Therefore, it is expected that the $[2 + 2]_{NC}$ products of both isothiazole and thiazole can be formed with mild thermal energies.

The natural orbital occupation numbers (NOON) of transition states are presented in the Table 2 in order to emphasize the multiconfigurational characters of current systems. The corresponding values of HOMO and LUMO of $TS_{isot}1$ are 1.654 and 0.346, respectively, indicating large diradical character of the transition states. Those of $TS_{thia}1$ also show similar values.

3.2.2 Concerted mechanism of [2 + 2]$_{CC}$ products

The $[2 + 2]_{CC}$ is the cycloaddition product between the C = C of molecules and the surface Si = Si dimer. Since it does not involve the nitrogen, the $[2 + 2]_{CC}$ is formed directly without the precursor state of Si–N dative adduct. In the case of isothiazole, the transition state ($TS_{isot}2$) directly connects the reactants and the $[2 + 2]_{CC}$ product ($P_{isot}2$) (see Fig. 3). The reaction barrier of this path is 27.9 kcal/mol, which is much higher than those $[2 + 2]_{NC}$ product ($P_{isot}1$) path. The NOON of $TS_{isot}2$ are 1.922, 1.122, 0.878 and 0.078. It shows nearly diradical electronic structures, clearly indicating the necessity of multiconfigurational wavefunctions. Although the $[2 + 2]_{CC}$ product ($P_{isot}2$) is more stable than $[2 + 2]_{NC}$ product ($P_{isot}1$), its high reaction barrier makes it kinetically the least favorable. The two Si–C bond lengths in $TS_{isot}2$ are calculated to be 2.13 and 2.98 Å, indicating an asymmetric transition state. The similar direct $[2 + 2]_{CC}$ path was also found in thiazole as shown in Fig. 3. The transition state ($TS_{thia}2$) directly connects the reactants and the $[2 + 2]_{CC}$ product ($P_{thia}2$). The predicted reaction barrier is 21.2 kcal/mol, which is still much higher than the $[2 + 2]_{NC}$ barrier.

In short, although the $[2 + 2]_{CC}$ cycloadditions of isothiazole and thiazole form slightly more stable products

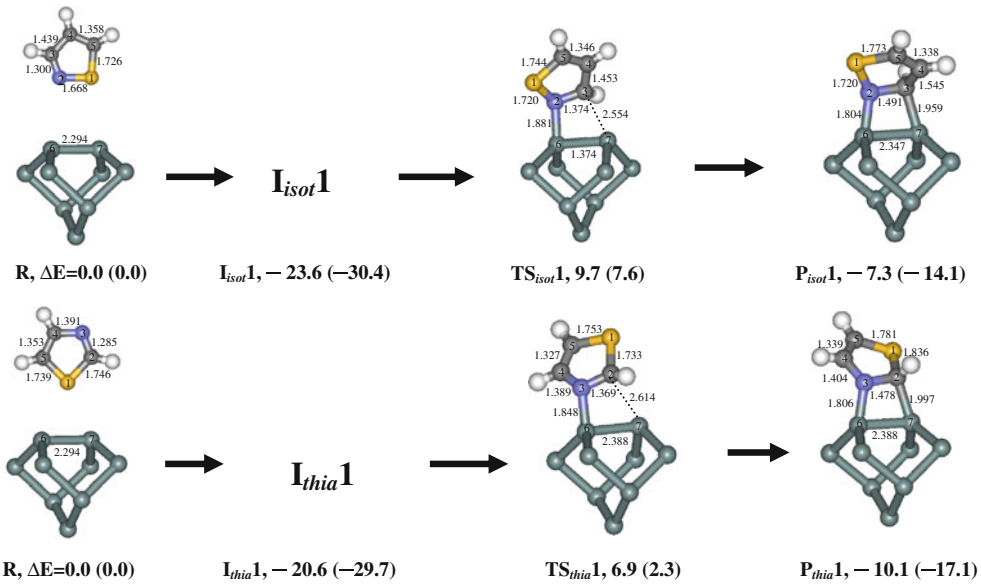

Fig. 2 The transition states and intermediates along the stepwise $[2 + 2]_{CN}$ cycloaddition channel of isothiazole and thiazole. Relative energies are obtained with SIMOMM:MRMP2/6-31G(d). The values in *parentheses* are obtained with SIMOMM:CASSCF/6-31G(d). Geometric data are from the CASSCF results

Table 2 Active space natural orbital occupation number (NOON) of the surface transition states

Transition states	Active space natural orbital occupation number (NOON)
$TS_{isot}1$	1.993, 1.986, 1.654, 0.346, 0.021
$TS_{thia}1$	1.998, 1.976, 1.611, 0.389, 0.026
$TS_{isot}2$	1.922, 1.122, 0.878, 0.078
$TS_{thia}2$	1.954, 1.101, 0.899, 0.046
$TS_{isot}3$	1.995, 1.978, 1.967, 1.666, 0.334, 0.035, 0.025
$TS_{thia}3$	1.999, 1.986, 1.980, 1.542, 0.458, 0.020, 0.015
TS_{ring}	1.998, 1.991, 1.987, 1.851, 1.431, 0.578, 0.155

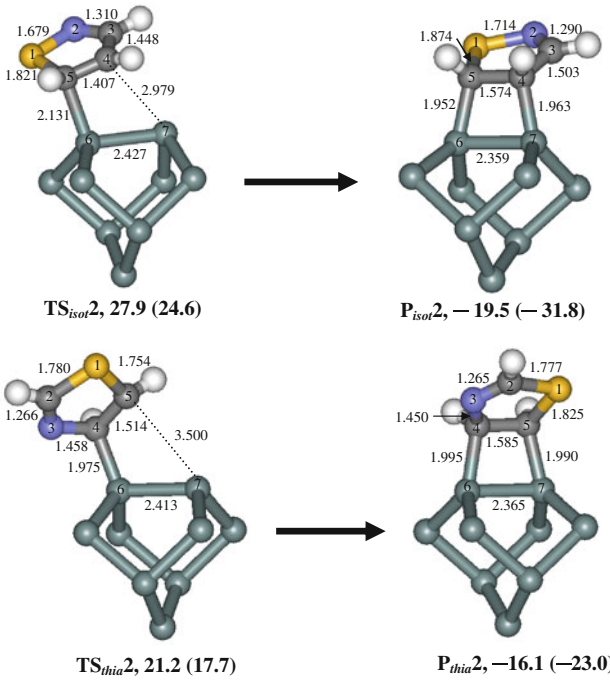

Fig. 3 The transition states and intermediates along the concerted $[2 + 2]_{CC}$ cycloaddition channel of isothiazole and thiazole. Relative energies are obtained with SIMOMM:MRMP2/6-31G(d). The values in *parentheses* are obtained with SIMOMM:CASSCF/6-31G(d). Geometric data are from the CASSCF results

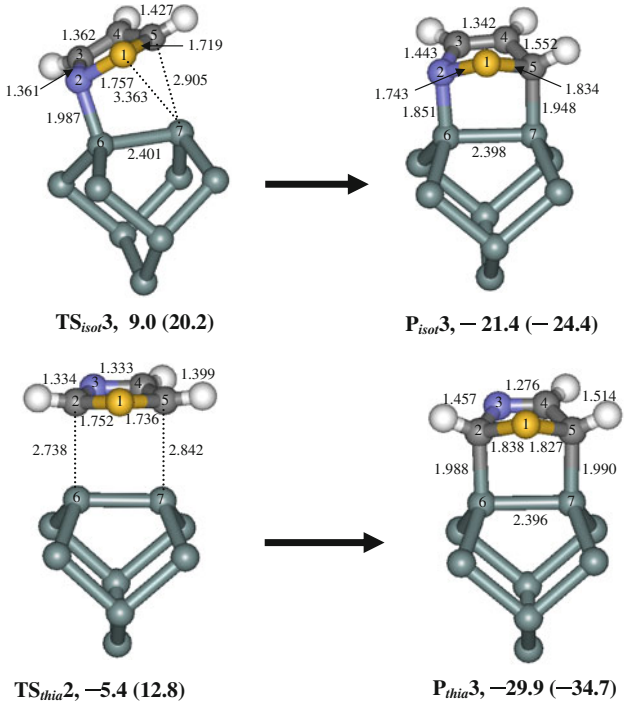

Fig. 4 The transition states and intermediates along the stepwise $[4 + 2]_{CN}$ cycloaddition channel of isothiazole and the concerted $[4 + 2]_{CC}$ cycloaddition channel of thiazole. Relative energies are obtained with SIMOMM:MRMP2/6-31G(d). The values in *parentheses* are obtained with SIMOMM:CASSCF/6-31G(d). Geometric data are from the CASSCF results

than $[2 + 2]_{NC}$ products, their large barriers make them kinetically less favorable.

3.3 Direct and indirect [4 + 2] cycloaddition reaction channels

3.3.1 Stepwise mechanism of $[4 + 2]_{NC}$ products

The formations of surface [4 + 2] products can be easily seen in many cases such as in the chemisorptions of benzene [20–31], 1,3-cyclohexadiene [15–19], pyridine [33], on the Si(100)−2 × 1 surface. Since the ordinary [4 + 2] cycloaddition reaction is symmetry-allowed, a small or zero reaction barrier to [4 + 2] products can be expected. Due to the two heteroatoms and the five-membered rings of isothiazole and thiazole, the [4 + 2] cycloaddition can only occur at 2,5 position. Consequently, the $[4 + 2]_{NC}$ cycloaddition of isothiazole should always involve one Si–N bond as shown in Fig. 4. Here, the subscript NC was added to emphasize the Si–N bond. The $[4 + 2]_{NC}$ product ($P_{isot}3$) forms heterogeneous di-σ-bonds onto the surface dimer through its 2 and 5 positions. The stability of the $[4 + 2]_{NC}$ product ($P_{isot}3$) is in between the stable Si–N dative adduct and less stable $[2 + 2]_{CC}$. Transition state $TS_{isot}3$ connects the Si–N adduct($I_{isot}1$) and the $[4 + 2]_{NC}$ product ($P_{isot}3$) with the reaction barrier of 9.0 kcal/mol. Although such large barrier of Diels–Alder is not uncommon [67–69], the value is sizable considering the symmetry-allowed [4 + 2] mechanism. Therefore, the $[4 + 2]_{NC}$ product ($P_{isot}3$) is not particularly favorable as compared to the initial Si–N dative-bond adduct. Structurally, the $TS_{isot}3$ has a very asymmetric configuration, since the Si_6-N_2 and Si_7-C_5 bond distances are calculated to be 1.99 and 2.91Å, which deviate from the ideal symmetric [4 + 2]

transition state structure. Since the $[4 + 2]_{NC}$ cycloaddition starts from the Si–N dative-bond adduct, its mechanism should be classified as a stepwise path.

3.3.2 *Concerted mechanism of $[4 + 2]_{CC}$ products*

In contrast to the $[4 + 2]_{NC}$, the corresponding $[4 + 2]_{CC}$ reaction of thiazole forms two Si–C bonds without involving nitrogen in a concerted fashion. Furthermore, the $[4 + 2]_{CC}$ reaction barrier of thiazole ($TS_{thia}3$) is predicted to be negligible -5.4 kcal/mol (see Fig. 4). In addition, the stabilization energy of $[4 + 2]_{CC}$ product ($P_{thia}3$) is predicted to be 29.9 kcal/mol, which is even more stable than the initial Si–N adduct, making the $[4 + 2]_{CC}$ path kinetically and thermodynamically the most favorable. Therefore, it is clear that the nature of $[4 + 2]_{CC}$ reaction of thiazole is strikingly different from that of isothiazole $[4 + 2]_{NC}$ channel.

At this point, it is interesting to compare the chemisorption behavior of thiazole with thiophene [66] on the same surface. Thiophene preferentially undergoes the [4 + 2] cycloaddition reaction forming di-σ-bonded 2,5-dihydrothiophene-like adspecies. This process is barrierless and exothermic with the predicted energies of -34.3 kcal/mol at B3LYP/6-31G(d) level of theory, which agrees well with those of thiazole.

3.4 Side reaction channel

3.4.1 *Reaction mechanism of N–S σ-bond cleavage in isothiazole*

One interesting side reaction of isothiazole is the N–S bond cleavage yielding a very stable surface product. The reaction starts from the Si–N adduct as in Fig. 5. By breaking

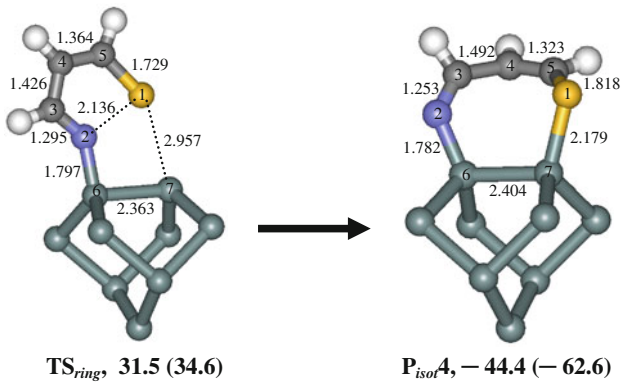

Fig. 5 The transition states and intermediates along the N–S σ-bond cleavage channel of isothiazole. Relative energies are obtained with SIMOMM:MRMP2/6-31G(d). The values in parentheses are obtained with SIMOMM:CASSCF/6-31G(d). Geometric data are from the CASSCF results

S_1-N_2 and making Si_7-S_1 bond, the transition state TS_{ring} connects the Si–N adduct ($I_{isot}1$) and the very stable 7-membered ring ($P_{isot}4$) with the reaction barrier of 31.5 kcal/mol, which is higher than the $[2 + 2]_{CN}$, $[2 + 2]_{CC}$, and $[4 + 2]_{CN}$ channels by 21.8, 3.6, and 22.5 kcal/mol, respectively. However, the resulted ring-opening product $P_{iso}4$ is the most stable with the stabilization energy of 44.4 kcal/mol. The similar ring opening was not found for thiazole. Therefore, it is a unique product of isothiazole. The $P_{iso}4$ can be formed if enough thermal energy can be provided. Once it is formed, it would not be converted to other product.

4 Conclusions

The surface reaction pathways of isothiazole and thiazole on Si(100)−2 × 1 surface were theoretically investigated. These two molecules commonly attached with Si(100) surface through Si–N dative-bond addition forming a stable initial adduct. In the case of isothiazole, $[2 + 2]_{NC}$ and $[4 + 2]_{NC}$ products can be formed from the initial Si–N dative-bond adduct as a stepwise fashion. These two reactions have relatively mild reaction barriers. However, the resulted products are not as stable as the initial Si–N adduct. A concerted direct $[2 + 2]_{CC}$ cycloaddition also exists. However, its large reaction barrier makes it kinetically the least accessible. Therefore, the Si–N dative-bond adduct of isothiazole is the most favorable initial product.

In the case of thiazole, the similar stepwise $[2 + 2]_{NC}$ and concerted $[2 + 2]_{CC}$ reaction were found. Most strikingly, a concerted $[4 + 2]_{CC}$ cycloaddition without involving the initial Si–N dative-bond adduct was found with no reaction barrier. It is due to the particular arrangement of the two heteroatoms of thiazole in such a way that two Si–C bonds can be formed. In the case of isothiazole, Si–N and Si–C bonds are formed. The nucleophilic N atom prefers addition reaction rather than cycloaddition, which would increase the reaction barriers in the case of isothiazole. Therefore, a direct reaction competition between the Si–N dative-bond adduct and the $[4 + 2]_{CC}$ can be only expected in thiazole. An interesting N–S bond cleavage reaction was found in the case of isothiazole. Although it has a large reaction barrier, the final outcome becomes very stable. Therefore, once N–S cleavage occurs, it would not be converted into other products.

In short, the geometric arrangements and heterogeneous electronegativity of these molecules significantly alter the well-known cycloaddition reactions, yielding striking differences in competition and selectivity of reaction channels.

Acknowledgments This work was supported by National Research Foundation of Korea (NRF) grant funded by the Korea government(MEST) (No. 2011-0001213 and No. 2011-0005032).

References

1. Choi CH, Gordon MS (2001) Chemistry on silicon surfaces. In: Rappoport Z, Apeloig Y (eds) The chemistry of organic silicon compounds, vol 3. Chap. 15. Wiley, New York, pp 821–852
2. Choi CH, Gordon MS (2004) Theoretical studies of silicon surface reactions with main group absorbates. In: Curtiss LA, Gordon MS (eds) Computational materials chemistry: methods and applications, chap 4. Kluwer Academic Publishers, Dordrecht, pp 125–190
3. Bilic A, Reimers J, Hush N (2006) Functionalization of semiconductor surfaces by organic layers: concerted cycloaddition versus stepwise free-radical reaction mechanism. In: Gruetter Peter, Rosei Federico, Hofer W (eds) Properties of single molecules on crystal surfaces, Chap 14. Imperial College Press, London
4. Woodward RB, Hoffmann R (1970) The conservation of orbital symmetry. Verlag Chemie, Weinheim
5. Nishijima M, Yoshinobu J, Tsuda H, Onchi M (1987) Surf Sci 192:383
6. Yoshinobu J, Tsuda H, Onchi M, Nishijima M (1987) J Chem Phys 87:7332
7. Taylor PA, Wallace RM, Cheng CC, Weinberg WH, Dresser MJ, Choyke WJ, Jr Yates JT (1992) J Am Chem Soc 114:6754
8. Li L, Tindall C, Takaoka O, Hasegawa Y, Sakurai T (1997) Phys Rev B 56:4648
9. Imamura Y, Morikawa Y, Yamasaki T, Nakasuji H (1995) Surf Sci 341:L1091
10. Liu Q, Hoffmann R (1995) J Am Chem Soc 117:4082
11. Rintelman JM, Gordon MS (2004) J Phys Chem B 108:7820
12. Liu H, Hamers RJ (1997) J Am Chem Soc 119:7593
13. Lopinski GP, Moffatt DJ, Wayner DDM, Wolkow RA (2000) J Am Chem Soc 122:3548
14. Lee HS, Choi CH, Gordon MS (2005) J Phys Chem B 109:5067
15. Konecny R, Doren D (1997) J Am Chem Soc 119:11098
16. Teplyakov AV, Kong MJ, Bent SF (1997) J Am Chem Soc 119:11100
17. Teplyakov AV, Kong MJ, Bent SF (1998) J Chem Phys 108:4599
18. Hovis JS, Liu HB, Hamers RJ (1998) J Phys Chem B 102:6873
19. Choi CH, Gordon MS (1999) J Am Chem Soc 121:11311
20. Taguchi Y, Fujisawa M, Takaoka T, Okada T, Nishijima M (1991) J Chem Phys 95:6870
21. Lopinski GP, Fortier TM, Moffatt DJ, Wolkow RA (1998) J Vac Sci Technol A 16:1037
22. Kong MJ, Teplyakov AV, Bent SF (1998) Surf Sci 411:286
23. Coutler SK, Hovis JS, Ellison MD, Hamers RJ (2000) J Vac Sci Technol A 18:1965
24. Craig BI (1995) Surf Sci 280:L279
25. Birkenheuer U, Gutdeutsch U, Rösch N (1998) Surf Sci 409:213
26. Wolkow RA, Lopinski GP, Moffatt DJ (1998) Surf Sci 416:L1107
27. Silvestrelli PL, Ancilotto F, Toigo F (2000) Phys Rev B 62:1596
28. Alavi S, Rousseau R, Seideman T (2000) J Chem Phys 113:4412
29. Jung Y, Gordon MS (2005) J Am Chem Soc 127:3131
30. Hofer WA, Fisher AJ, Lopinski GP, Wolkow RA (2001) Phys Rev B 61:085314
31. Alavi S, Rousseau R, Patitsas SN, Lopinski GP, Wolkow RA, Seideman T (2000) Phys Rev Lett 85:5327
32. Choi CH, Gordon MS (2002) J Am Chem Soc 124:6162
33. Tao F, Qiao MH, Wang ZH, Xu GQ (2003) J Phys Chem B 107:6384
34. Tao F, Bernasek SL (2007) J Am Chem Soc 129:4815
35. Hehre WJ, Ditchfield R, Pople JA (1972) J Chem Phys 56:2257
36. Sunberg KR, Ruedenberg K (1976) Quantum Science. In: Goscinski O, Linderberg J, Ohrn Y (eds) Calais JL. New York, Plenum
37. Cheung LM, Sunberg KR, Ruedenberg K (1979) Int J Quantum Chem 16:1103
38. Ruedenberg K, Schmidt M, Gilbert MM, Elbert ST (1982) Chem Phys 71:41
39. Roos BO, Taylor P, Siegbahn PE (1980) Chem Phys 48:157
40. Schmidt MW, Gordon MS (1998) Annu Rev Phys Chem 49:233
41. Warner HJ (1996) Mol Phys 89:645
42. Glaesemann KR, Gordon MS, Nakano H (1999) Phys Chem Chem Phys 1:967
43. Nakano H (1993) J Chem Phys 99:7983
44. Nakano H (1993) Chem Phys Lett 207:372
45. Schmidt MW, Baldridge KK, Boatz JA, Elbert ST, Gordon MS, Jensen JH, Koseki S, Matsunaga N, Nguyen KA, Su S, Windus TL, Dupuis M, JAJr Montgomery (1993) J Comput Chem 14:1347
46. Fletcher GD, Schmidt MW, Gordon MS (1999) Adv Chem Phys 110:267
47. Shoemaker JR, Burgraff LW, Gordon MS (1999) J Phys Chem A 103:3245
48. Choi CH, Liu D, Evans JW, Gordon MS (2002) J Am Chem Soc 124:8730
49. Ghosh MK, Choi CH (2010) J Phys Chem C 114:14187
50. Ghosh MK, Choi CH (2006) Chem Phys Lett 426:365
51. Ghosh MK, Choi CH (2008) Chem Phys Lett 457:69
52. Cho J, Choi CH (2008) J Phys Chem C 112:6907
53. Ghosh MK, Choi CH (2006) J Phys Chem B 110:11277
54. Ghosh MK, Sarker MIM, Choi CH (2008) J Phys Chem C 112:9327
55. Ghosh MK, Choi CH (2008) Chem Phys Lett 461:249
56. Cho J, Ghosh MK, Choi CH (2009) Bull Korean Chem Soc 30:1805
57. Zorn DD, Albao MA, Evans JW, Gordon MS (2009) J Phys Chem C 113:7277
58. Lee HS, Choi CH (2008) Theor Chem Acc 120:79
59. Tamura H, Gordon MS (2003) J Chem Phys 119:10318
60. Zapol P, Curtiss LA, Tamura H, Gordon MS (2004) Theoretical studies of growth reactions on diamond surfaces. In: Curtiss LA, Gordon MS (eds) Computational materials chemistry: methods and applications. Kluwer Academic Publishers, Boston, pp 266–307
61. Allinger NL, Yuh YH, Lii JH (1989) J Am Chem Soc 111:8551
62. Lii JH, Allinger NL (1989) J Am Chem Soc 111:8566
63. Lii JH, Allinger NL (1989) J Am Chem Soc 111:8576
64. Lu X, Xu X, Wu J, Wang N, Zhang Q (2002) New J Chem 26:160
65. Lim C, Choi CH (2003) J Phys Chem B 107:6853
66. Lu X, Xu X, Wang N, Zhang Q, Lin MC (2001) J Phys Chem B 105:10069
67. Beno BR, Houk KN, Singleton DA (1996) J Am Chem Soc 118:9984
68. Garcia JI, Martinez-Merino V, Mayoral JA, Salvatella L (1998) J Am Chem Soc 120:2415
69. Paton RS, Mackey JL, Kim WH, Lee JH, Danishefsky SJ, Houk KN (2010) J Am Chem Soc 132:9335